

SLIP PREDICTION FOR PLANETARY ROVER TRAVERSABILITY ASSESSMENT USING ORBITAL IMAGERY

Gabrielle Hedrick^a, Masahiro Ono^b

^aWest Virginia University, 1306 Evansdale Drive, PO Box 6106 Morgantown, West Virginia 26506-6106

^bJet Propulsion Laboratory, California Institute of Technology, 4800 Oak Grove Dr, Pasadena, CA 91109
glc0006@mix.wvu.edu, masahiro.ono@jpl.nasa.gov

Abstract

Terrain trafficability (and consequently, vehicle traversability) is an important factor in planetary rover missions. Terrain trafficability is defined as the ability of a terrain to sustain the traversal of a mobile vehicle (Papadakis, 2013; Muro, 2004). It depends on the rover itself and factors such as terrain properties and topography. Currently, the trafficability assessment mostly depends on on-board images taken from the previous sol (Martian day), with which making a reliable assessment on the surface beyond a few tens of meters from the current position is difficult. Orbital images are also used to assess the drivability beyond this distance, but it is hard to make a reliable prediction on key trafficability metrics, such as slip, due to its limited resolution. To improve predictions over extensive distances and to support ground assessment of the terrain, this paper proposes a method to support slip assessment from thermal inertia measured by orbital observations. More specifically, the proposed model takes thermal inertia maps and digital elevation models as inputs and predicts whether slip is less than 30% or greater. Thermal inertia translates the ability of a material to store heat during the day and release it at night, and depends on various terrain properties (e.g., grain size, conductivity), that could affect trafficability. In general, the lower the thermal inertia, the lower the trafficability, and vice versa (Cunningham, 2017). These results confirms that thermal inertia plays an important role in predicting slip and could improve terrain trafficability assessment significantly. Other data sets were also tested in combination with thermal inertia and slope, such as terrain types and rock abundance, but it did not significantly change the performance of the model. The contribution of this work is to incorporate thermal inertia to slip prediction, producing a model that can give results covering great distances, and could be key to safer missions.

Keywords: Slip Prediction, Mars Rover, Trafficability, Orbital Data, Thermal Inertia, Slope

1. Introduction

Terrain trafficability is an important factor in all planetary rovers, especially as future surface missions become more complex and aim at going further into the solar system (Lorenz et al., 2018). These missions require autonomy in robotics as it would enable driving beyond line-of-sight (i.e., beyond what is seen on images received from the planet's surface), ensure safety at every step, and allow more complex designs to be put together with restricted budget and staffing (Fong et al., 2017). Trafficability is defined as the ability for a given terrain to sustain the traversal of a mobile robot without reaching failure and involves studying the robot's response to the terrain it is driven on (Papadakis, 2013). While trafficability is a terrain characteristic, this work also mentions traversability, which is the ability of a vehicle to traverse a terrain. The two are used throughout this paper, depending whether the rover or the terrain is considered.

For planetary surfaces, the terrain is not always known and research has focused for years on ways to assess trafficability and traversability with limited information. After the loss of the rover Spirit at Gusev Crater in 2010, it has become even more important to understand terrain properties and how vehicles interact with the ground on remote worlds. Spirit traversed compacted terrain at the beginning while on Gusev plains,

15 however, upon arriving at the Columbia Hills, it encountered highly deformable sulfate rich soil that made
16 traversability a challenge (Johnson et al., 2015). Moreover, these soils were covered in basaltic sand, making
17 them invisible to the team planning the traverse. The rover underwent high sinkage (up to 10 cm), and the
18 failure of the right front wheel actuator made the traverse even worse as Spirit was forced to drag its wheel
19 along. It eventually got embedded in a sand filled crater when the left side of the rover tilted into the crater
20 and the wheel got stuck (Johnson et al., 2015). Failure to extricate Spirit led to the end of its mission in
21 2010. Opportunity encountered high wheel sinkage situations as well, at Endeavour Crater, when it came
22 across the Purgatory ripple field (Arvidson et al., 2011) and Curiosity experienced mobility difficulties with
23 wheel damage (holes and dents) from roving on sharp rocks (Arvidson et al., 2017).

24 Terramechanics, i.e., vehicle-terrain interaction mechanics, has been identified as a way to assess traffica-
25 bility given the constraints of planetary missions, and more specifically, the interaction of the rover's wheels
26 with the surface can potentially provide answers to the question of trafficability. Understanding the terrain
27 and its interaction with Curiosity's wheels may have prevented any damage, and there is a recognized need
28 to incorporate terramechanics to planning to prevent mobility issues (Arvidson, 2014). Early in the applica-
29 tion of terramechanics to planetary rovers, some variables have been identified as necessary for exploration
30 missions, such as slip (Ding et al., 2011). The authors point out the necessity of estimating the amount of
31 slip encountered by the rover, given the limited onboard computational resources. Slip is highly related to
32 terrain trafficability: limited slip could indicate traversable areas, and high slip could point to difficult if
33 not untraversable areas. Most importantly, high slip can lead to the rover getting embedded, temporarily
34 trapped, as did Curiosity on sol 672 (Bouguelia et al., 2017), or not being able to recover, as demonstrated
35 by Spirit (Johnson et al., 2015).

36 As NASA prepares for its very next rover mission to Mars, Mars 2020, it is important to understand how
37 the Perseverance Rover would potentially behave when roving on the regolith at Jezero Crater, the chosen
38 landing site (NASA, 2018). The goal of this research is to assess slip using orbital imagery available, leading
39 to prediction over extensive areas that could support ground-based terrain trafficability assessment. This
40 paper is organized as follows: after detailing related research, the problem statement of this work will be
41 presented, followed by the technical approach. Results and conclusion will be presented next.

42 2. Related Work

43 As previously mentioned, terrain trafficability is an important factor to take into consideration in prepa-
44 ration for the next Mars mission, Mars 2020. During the lunar era, missions such as Lunakhod and Apollo
45 sent instruments to the Moon to assess the terrain and its trafficability (Zacny et al., 2010). Since, research
46 has been published that uses terramechanics to assess the terrain in real time, and includes a wide range of
47 techniques, from the use of wheels and sensors to actual instruments (Chhaniyara et al., 2012). For example,
48 a terrain classifier has been proposed that uses the vibrations induced in the vehicle by the wheel-terrain
49 interaction during a drive (Brooks & Iagnemma, 2005) to identify terrains and assess their safety with re-
50 gards to driving. Another model was proposed to identify key terrain properties using on-board sensors and
51 estimate traversability from these parameters (Iagnemma et al., 2004). Both models assess traversability
52 while driving, which makes predictability for long distances a challenge. To remedy this issue, other methods
53 have been proposed, such as simulations offline of traverses on a user-defined terrain with a software called
54 ARTEMIS (Adams-based Rover Terramechanics and Mobility Interaction Simulator). This software has
55 been validated with a single wheel experiment (Senatore et al., 2014), as well as tests in the JPL Mars Yard
56 and field experiments in the Mojave Desert (Zhou et al., 2014, 2017). It has then been used to simulate
57 traverses for the Opportunity and Curiosity rovers. However, since orbital imagery is usually not enough to
58 fully characterize a terrain (Gaines et al., 2016), this method requires ground data and is therefore limited
59 to the few tens of meters ahead of the rover, where terrain parameters can be assessed more precisely. More
60 recently, several authors have looked into predicting better traverse performance by taking into account or-
61 bital data such as HiRISE (High Resolution Imaging Science Experiment) or slope in a software called Mars
62 Terrain Traversability Tool (Ono et al., 2016). MTTT uses a terrain classifier, Soil Property and Object
63 Classification (SPOC) that analyses HiRISE images to classify different terrains into different categories

(Rothrock et al., 2016). These terrain types are coupled with rock abundance (Cumulative Fractional Area (Golombek & Rapp, 1996) or CFA), hazards and slope to predict rover speed (Ono et al., 2016).

Some other terrain trafficability prediction models use slip to directly assess the safety of driving (Ding et al., 2009). Slip is an important aspect of terrain trafficability and has been the subject of many studies (Senatore et al., 2014; Johnson et al., 2015). It is a response of the wheels driving on a surface (e.g., sandy, steep) and is highly related to the terrain type. Intuitively, high slip lowers trafficability, as seen with Spirit when its wheels reached 100% slip (Johnson et al., 2015), and vice-versa. Tests to analyze slip behaviors for MERs on different slopes were conducted in the laboratory (Biesiadecki et al., 2006). Several models for slip have been proposed, especially in the foundation work of terramechanics (Bekker, 1969; Wong et al., 1989), but it is not until later that predicting slip has been attempted and used as a mean of assessing terrain trafficability. For example, some authors have proposed a model that utilizes on-board cameras to remotely classify terrains, predict slip and plan the path given the three terrain categories: traversable, not traversable, and uncertain. This system has been specifically intended for planetary rovers after seeing the difficulties encountered on Mars (Helmick et al., 2008). Another prediction model uses visual information from the rover itself (e.g., stereo images) to give an estimate of slip on forthcoming terrains (Angelova et al., 2007; Angelova, 2008) to help identify safer paths. Later, thermal inertia has been suggested as a tool to assess slip, using both the Ground Temperature Sensor (GTS) onboard Curiosity (Sebastián et al., 2010) and the Thermal Emission Imaging Spectrometer (THEMIS) onboard the satellite Mars Odyssey (Christensen et al., 2004). The results from rover-based and orbital analysis show that thermal inertia greatly helps in improving slip predictions given slope, and that overall, lower slip is correlated with decreased thermal inertia (Cunningham, 2017). Most of slip prediction methods, however, utilize on-board resources and do not rely solely on orbital imagery.

3. Problem statement and contribution

The main goal is to provide a method that predicts ranges of slip for a Mars rover in order to facilitate and support ground terrain trafficability assessment, using only information available *a priori*, i.e., orbital data. Terrain information publicly available includes topography, (Digital Elevation Models or DEMs via HiRISE, the High Resolution Imaging Science Experiment), thermal inertia and slip data for both Mars Exploration Rovers (MER), i.e., Spirit (MERa) and Opportunity (MERb). In addition, other information available for this study include rock abundance (Golombek & Rapp, 1996) or CFA (Cumulative Fractional Area) and terrain types (Rothrock et al., 2016); however, these information are only available at Gusev Crater (MERa landing site). The main constraint for this research is the limited amount of data available, that is, the analysis is limited to the length of the traverses, the orbital coverage over the traverses, and the slip checks performed along the way. The main challenge is to reconcile the data to obtain values of slope, thermal inertia and slip, as well as terrain types and CFA when available, at measurement points. It is assumed that this method can be applied to other landing sites on Mars for other rovers (e.g., Perseverance).

The contributions of this work are the following: 1) to propose a method that allows for direct prediction of slip using orbital data only; 2) to provide a mean of predicting slip that can support ground terrain assessment; and 3) to give trafficability information over extended distances, as long as the orbital coverage is available, which means that a path can be analyzed with greater certainty prior to the mission landing.

4. Technical approach

4.0.1. Orbital Data

Thermal inertia can be used for terrain trafficability analysis as it brings information about the surface and subsurface. It is derived from the Mars Odyssey Thermal Emission Imaging System (THEMIS) nighttime temperatures (Ferguson et al., 2006) and depends on several factors including particle size, degree of induration, rock abundance and exposure of bedrock at the subsurface (within a few centimeters of the

109 surface). It translates the ability of a material to store heat during the day and release it at night (Putzig
110 et al., 2005) and is defined as follows:

$$I = \sqrt{k\rho c} \quad (1)$$

111 Where I is the thermal inertia in thermal inertia unit (TIU, $1 \text{ TIU} = 1 \text{ Jm}^{-2}\text{K}^{-1}\text{s}^{-1/2}$), k is the bulk
112 thermal conductivity, ρ is the bulk density and c is the specific heat of the surface layer (up to a few
113 centimeters below the surface (Putzig et al., 2005)). In general, given that thermal inertia is directly
114 proportional to the bulk density and therefore compaction and bearing strength, low values are associated
115 with deep sand, leading to harder conditions for a rover to drive, whereas high thermal inertia translates
116 into indurated material such as bedrock. This implies that the rover would have less difficulty driving on
117 terrains displaying higher values of thermal inertia (Cunningham, 2017). The thermal inertia data set has a
118 resolution of 100 m/pixel (Ferguson et al., 2006). Thermal inertia has been used in the past to understand
119 surface properties (Putzig & Mellon, 2007) and has been considered for slip predictability and trafficability
120 assessment (Cunningham, 2017).

121 Slope also plays a significant role in terrain trafficability. The Mars Exploration Rovers (MERs) avoided
122 slope greater than 30° due to potential sliding on steeper slope (Biesiadecki et al., 2006). Testing has been
123 conducted to understand trafficability on different slopes for Spirit and Opportunity (Lindemann & Voorhees,
124 2005) and Curiosity (Heverly et al., 2013). Slope is obtained from Digital Elevation Models (DEMs) over
125 selected areas, which have a resolution of 1m/pixel. Slope is derived from the gradient of the height from
126 the DEM times the heading angle in the rover's direction as shown in Eq.(2).

$$S = \begin{pmatrix} \frac{\partial h}{\partial x} \\ \frac{\partial h}{\partial y} \end{pmatrix} \cdot \begin{pmatrix} \cos\theta \\ \sin\theta \end{pmatrix} \quad (2)$$

127 Where h is the height given by the DEM, (x, y) are the coordinates of the location for which slope is
128 calculated (pixel of 1 square meter), and θ is the heading angle. The slope is calculated at the (x, y) location
129 by deriving the gradient for the average height over 9 pixels (the pixel (x, y) and the 8 surrounding pixels).

130 In addition to thermal inertia and slope available at both sites, the SPOC software generated a terrain
131 type map for Gusev Crater (Rothrock et al., 2016) and the associated CFA coverage (Golombek & Rapp,
132 1996) was made available for this study.

133 4.1. Principal Component Analysis (PCA)

Table 1: Principal Component Analysis (PCA) results showing PC (Principal Components) 1 to 4 with the contribution of each variable (in %).

	PC1	PC2	PC3	PC4
Variance explained	46.51%	28.21%	14.83%	10.46%
Thermal inertia	6.250%	65.62%	14.78%	13.35%
Slope	19.82%	30.70%	44.60%	48.80%
Terrain types	34.94%	0.9800%	40.55%	23.53%
CFA	38.99%	2.710%	0.07450%	58.23%

134 To better understand the role of slope and thermal inertia, a Principal Component Analysis (PCA) on
135 all four variables (thermal inertia, slope, terrain types and CFA), centered and standardized, is performed
136 at Gusev Crater. It revealed that the first three components contribute to 89.54% of the data, almost 90%,
137 and the first two alone contributes to 74.71% of the data, almost 75%. The biplot shown in Fig.1 shows that
138 if terrain types and CFA contribute the most to PC1, slope and thermal inertia contribute the most to PC2
139 and most importantly, to the total explained variance by dimension one and two, at 53.70% and 39.23%
140 respectively (Fig.1). Thermal inertia and slope are thus retained as the main contributing variables and the
141 predictors needed for slip analysis.

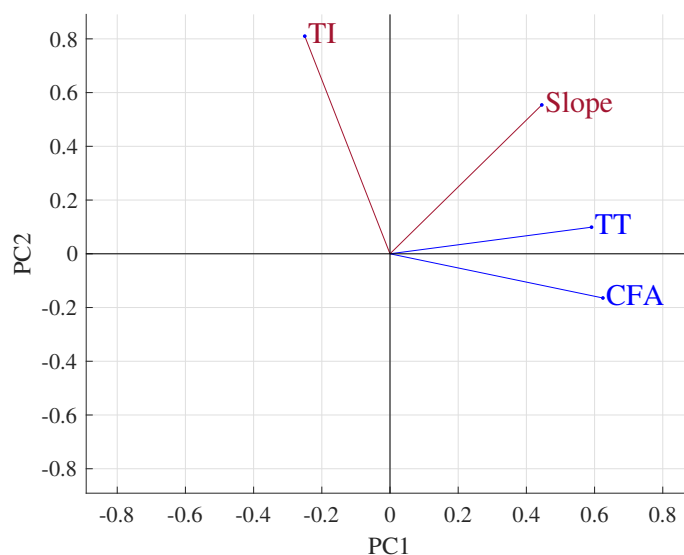


Fig. 1: Biplot showing the contribution of each variable to the first two PCs that explain 75% of the data. TI: thermal inertia; TT: terrain types; CFA: cumulative fractional area.

142 4.2. Data points available

143 The data are taken from both the Opportunity and Spirit rovers, at Meridiani Planum and Gusev Crater,
 144 respectively. Slip was recorded only when Visual Odometry (VO) was enabled - called “slip checks” (Maimone
 145 et al., 2007). However, VO was not always an option since it did not allow for fast speed (Biesiadecki et al.,
 146 2007), and consequently, few data points were available for this study, as shown in 2. 2073 data points were
 147 collected for Spirit (MER A, Fig.2b) and 3250 for Opportunity (MER B, Fig.2a, processed DEM coverage
 148 is not available everywhere at Meridiani Planum).

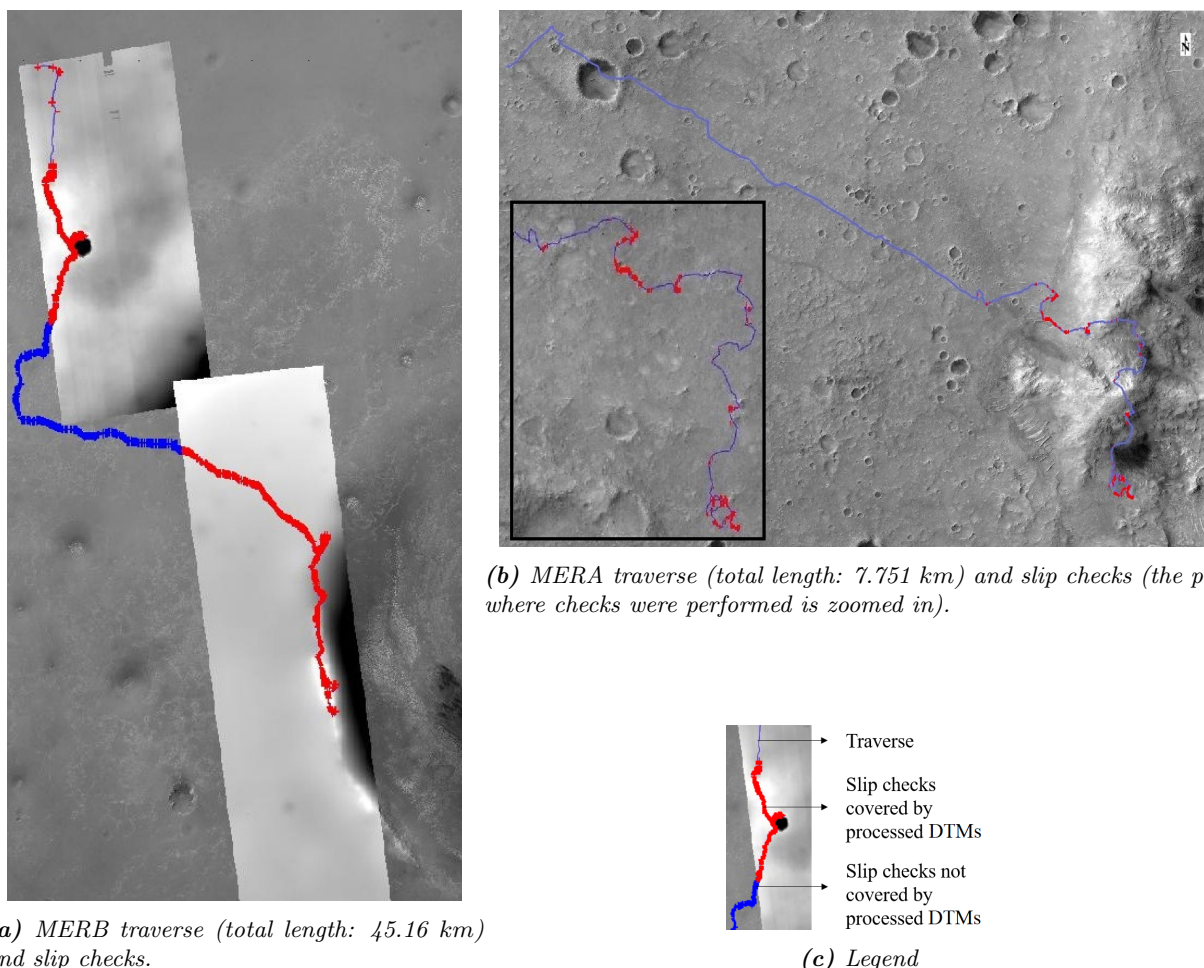
149 4.3. Data processing

150 If slope has been identified for a long time as a factor for slip experienced by rovers (Bouguelia et al.,
 151 2017), the role of thermal inertia was not as clearly defined until recently (Cunningham, 2017). It is related
 152 to terrain properties as shown in section 4.0.1 and is important with regards to predicting slip.

153 The slope and thermal data were combined to train a classifier to predict ranges of slip: lower than 30%
 154 or higher than 30%. This threshold was taken from a similar classification used in Bouguelia et al. (2017)
 155 with classes medium slip (30 – 60%) and high slip (> 60%) combined into one category. While their work
 156 focuses on tracking ranges of slip from ground data and rover behavior, this research aims at producing a
 157 classifier that will allow slip prediction exclusively from orbit. In order to obtain the value for slope and
 158 thermal inertia at the location of the slip value, the raw data were georeferenced and longitude and latitude
 159 for each pixel of the maps were obtained. Similarly, slip checks coordinates in terms of latitude and longitude
 160 were computed along the traverse. And finally, the height from the DEM at each pixel was converted to slope
 161 by averaging the values over the height surrounding pixels and deriving the gradient in the rover direction.

162 4.4. Classifier training

163 Once the matrix of slope, thermal inertia and slip values at measurement locations was obtained, the
 164 data were prepared for training a classifier. It involved converting the slip data to two categories, that is,
 165 “low” and “high”, which correspond to 0 – 30% and above 30%, respectively. Slope and thermal inertia were
 166 also categorized into different classes. Slope categories were taken from Ono et al. (2018), where the ranges
 167 considered are 0 – 5°, 5 – 10°, 10 – 15°, 15 – 20°, 20 – 15° and above 25°. However, slope above 15° are



(a) MERB traverse (total length: 45.16 km) and slip checks.

(b) MERA traverse (total length: 7.751 km) and slip checks (the part where checks were performed is zoomed in).

(c) Legend

Fig. 2: Data points available for this study. (a) Slip checks with orbital coverage available for Opportunity (in red, B data kept for validation). (b) Slip checks with orbital coverage available for Spirit (in red, A data used for training). (c) Legend.

168 already considered complicated terrain (Biesiadecki et al., 2007), therefore only 3 categories of slope were
 169 considered: $0 - 10^\circ$, $10 - 15^\circ$ and above 15° . Each category was then split to account for the direction of
 170 the slope, that is, up or down. Thermal inertia was also divided into categories, with high thermal inertia
 171 above 200 TIU and low thermal inertia below 200 TIU.

172 Multiple classification methods were considered, including: trees, naive Bayes or nearest neighbors. The
 173 Spirit data were used for training the classifier (referred to as the A set) and the data from Opportunity were
 174 used for validating the trained classifier (referred to as the B set). However, it should be noted that among
 175 the 2 categories, both for the training data and the testing data, the first category is over-represented. For
 176 all data sets combined, there is a total of 5323 slip check points with the required orbital coverage, with 4491
 177 belonging to class “low” (84.4%) and only 832 belonging to class “high” (15.6%). Among the A set (from
 178 Spirit’s traverse), 1600 are category “low” (77.2%) and 473 are “high” (22.8%). Among the B set (from
 179 Opportunity’s traverse), 2891 are “low” (89%) and 354 are “high” (11%). This led to an imbalanced class
 180 problem for training the classifier that needed to be taken into account. There are ways to handle the class
 181 imbalance so that the model does not get biased towards the most represented category, including tuning the
 182 misclassification cost matrix or using boosting and/or sampling methods (Weiss, 2004) such as AdaBoost
 183 (Adaptive Boosting) (Liu et al., 2008) or RUS (Random Under Sampling). Authors have also proposed to

184 combine both sampling and boosting methods to improve even further the performance of a classifier when
 185 handling imbalanced data, called RUSboost (Seiffert et al., 2008). When compared to different algorithms,
 186 RUSboost was proved to perform better than sampling or boosting methods alone (Seiffert et al., 2009).

187 **5. Results**

188 *5.1. Classifier training*

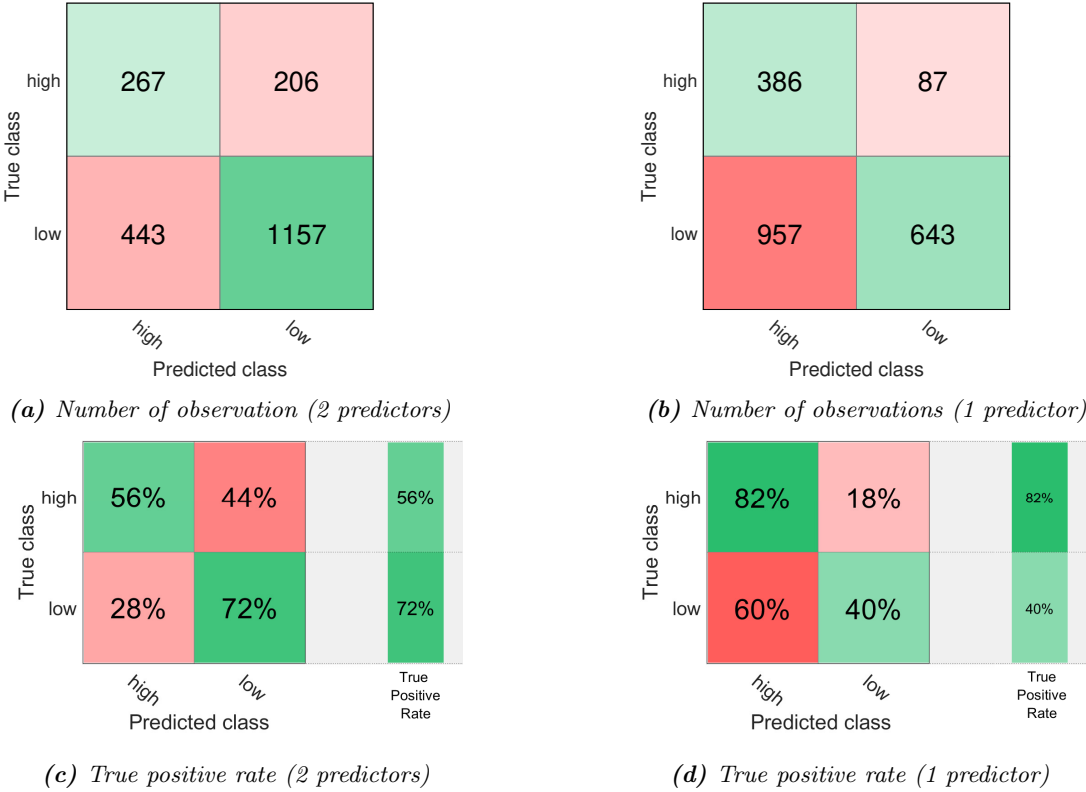


Fig. 3: Confusion matrices showing the performance of the trained model on data set B2.

189 As a result of the PCA analysis in section 4.1, the classifier was trained using the variables contributing
 190 the most to the explained variance, that is, slope and thermal inertia. The best results were obtained using a
 191 decision tree classifier with a RUSboost algorithm and a penalty cost of 5 for “low” misclassified as “high” and
 192 1.5 for “high” misclassified as “low”. The classifier algorithms was first chosen based on overall performance
 193 and has the following characteristics: maximum number of split is 50 and the number of learners is set to 30.
 194 The same model was then trained without thermal inertia as a predictor. The performance of the classifier
 195 is presented in Fig.3. The overall performance is 68.7% for the classifier with two predictors and drops to
 196 49.6% when using only slope as a predictor. The overall performance the trained models tends to confirm
 197 the results from the PCA analysis, demonstrating the need for thermal inertia. Low slip prediction increases
 198 from 40% to 72% when adding thermal inertia; however, high slip prediction shows better results when the
 199 algorithm is trained with one predictor only. Overall, the conclusion is that thermal data are an important
 200 component of slip prediction analysis.

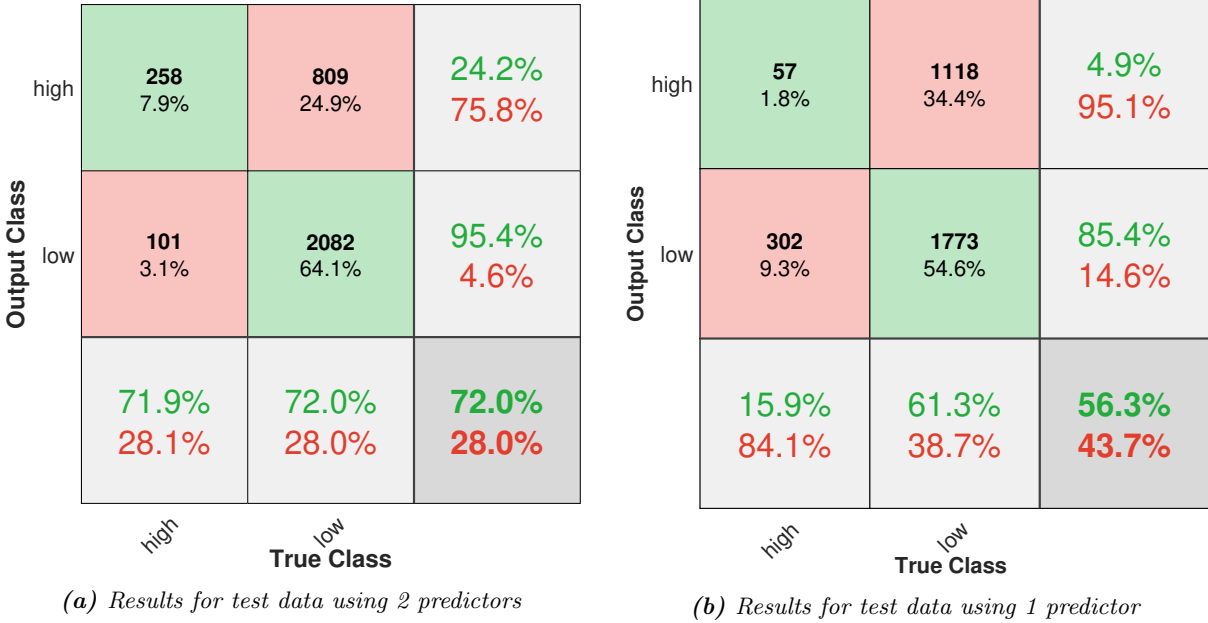


Fig. 4: Confusion matrices on test data set B for (a) model with 2 predictors and (b) model with 1 predictor.

201 5.2. Validation on new data

202 All data from the B set were used to test the trained classifier. The results are presented in Fig.4 where
 203 the algorithm using thermal inertia and slope as predictors (Fig.4a) and the model taking only slope as
 204 predictor (Fig.4b) are tested.

205 The results show that the overall performance of the model is good (72.0%) and decreases significantly
 206 (down to 56.3%) when using only slope as a predictor. This confirms that thermal inertia is an important
 207 value to consider when predicting slip. The model is capable of predicting low slip and high slip pretty well,
 208 scoring 71.9% and 72.0% of the data, respectively. When thermal inertia is dropped and slope only is used,
 209 the model goes barely above average for low slip data, predicting only 61.3%, and does not even correctly
 210 categorize more than a quarter of the high slip data, scoring only 15.9%. The model trained with only slope
 211 as predictor therefore performs poorly and these results reinforce previous conclusions: thermal inertia is a
 212 valuable asset to the prediction of mobility performance.

213 6. Conclusion

214 This work implemented a classifier that takes orbital data as input to predict whether slip will be greater
 215 or less than 30% over chosen areas. By comparing the same type of classifier with difference input, it
 216 is established that thermal inertia plays a key role in predicting the amount of slip the rover is likely to
 217 experience, as suggested in Cunningham (2017). Indeed, thermal inertia gives valuable insight into the first
 218 few centimeters of the terrain, which greatly affect the rover performance. When paired with slope, thermal
 219 inertia is able to predict with good accuracy the range of slip a vehicle will experience on a given terrain.

220 Future work includes studying the performance of this classifier at other landing sites, such as Gale
 221 Crater, and improving its efficiency with the additional information.

222 Acknowledgement

223 The authors would like to thank Heather Justice for all the help she provided in getting and understanding
 224 the raw data from MER and making this research possible. This research is partially funded by the Benjamin
 225 M. Statler fellowship. It was carried out in part at the Jet Propulsion Laboratory, California Institute of
 226 Technology, under a contract with the National Aeronautics and Space Administration (80NM0018D0004).

227 References

- 228 Angelova, A. (2008). *Visual prediction of rover slip: learning algorithms and field experiments*. Technical
 229 Report CALIFORNIA INST OF TECH PASADENA.
- 230 Angelova, A., Matthies, L., Helmick, D., & Perona, P. (2007). Slip prediction using visual information, .
- 231 Arvidson, R., DeGrosse Jr, P., Grotzinger, J., Heverly, M., Shechet, J., Moreland, S., Newby, M., Stein, N.,
 232 Steffy, A., Zhou, F. et al. (2017). Relating geologic units and mobility system kinematics contributing to
 233 curiosity wheel damage at gale crater, mars. *Journal of Terramechanics*, *73*, 73–93.
- 234 Arvidson, R. E. (2014). Roving on mars with opportunity and curiosity: terramechanics and terrain prop-
 235 erties. In *Earth and Space 2014* (pp. 165–173).
- 236 Arvidson, R. E., Ashley, J. W., Bell, J., Chojnacki, M., Cohen, J., Economou, T., Farrand, W. H., Ferguson,
 237 R., Fleischer, I., Geissler, P. et al. (2011). Opportunity mars rover mission: Overview and selected results
 238 from purgatory ripple to traverses to endeavour crater. *Journal of Geophysical Research: Planets*, *116*.
- 239 Bekker, M. G. (1969). *Introduction to Terrain-Vehicle Systems. Part I: The Terrain. Part II: The Vehicle*.
 240 Technical Report MICHIGAN UNIV ANN ARBOR.
- 241 Biesiadecki, J. J., Baumgartner, E. T., Bonitz, R. G., Cooper, B., Hartman, F. R., Leger, P. C., Maimone,
 242 M. W., Maxwell, S. A., Trebi-Ollennu, A., Tunstel, E. W. et al. (2006). Mars exploration rover surface
 243 operations: Driving opportunity at meridiani planum. *IEEE robotics & automation magazine*, *13*, 63–71.
- 244 Biesiadecki, J. J., Leger, P. C., & Maimone, M. W. (2007). Tradeoffs between directed and autonomous
 245 driving on the mars exploration rovers. *The International Journal of Robotics Research*, *26*, 91–104.
- 246 Bouguelia, M.-R., Gonzalez, R., Iagnemma, K., & Byttner, S. (2017). Unsupervised classification of slip
 247 events for planetary exploration rovers. *Journal of Terramechanics*, *73*, 95–106.
- 248 Brooks, C. A., & Iagnemma, K. (2005). Vibration-based terrain classification for planetary exploration
 249 rovers. *IEEE Transactions on Robotics*, *21*, 1185–1191.
- 250 Chhaniyara, S., Brunskill, C., Yeomans, B., Matthews, M., Saaj, C., Ransom, S., & Richter, L. (2012).
 251 Terrain trafficability analysis and soil mechanical property identification for planetary rovers: A survey.
 252 *Journal of Terramechanics*, *49*, 115–128.
- 253 Christensen, P. R., Jakosky, B. M., Kieffer, H. H., Malin, M. C., McSween, H. Y., Nealon, K., Mehall, G. L.,
 254 Silverman, S. H., Ferry, S., Caplinger, M. et al. (2004). The thermal emission imaging system (themis)
 255 for the mars 2001 odyssey mission. *Space Science Reviews*, *110*, 85–130.
- 256 Cunningham, C. (2017). *Improving Prediction of Traversability for Planetary Rovers Using Thermal Imag-*
 257 *ing*. Ph.D. thesis Carnegie Mellon University.
- 258 Ding, L., Deng, Z., Gao, H., Nagatani, K., & Yoshida, K. (2011). Planetary rovers’ wheel–soil interaction
 259 mechanics: new challenges and applications for wheeled mobile robots. *Intelligent Service Robotics*, *4*,
 260 17–38.

- 261 Ding, L., Gao, H., Deng, Z., Yoshida, K., & Nagatani, K. (2009). Slip ratio for lugged wheel of planetary rover
262 in deformable soil: definition and estimation. In *2009 IEEE/RSJ International Conference on Intelligent
263 Robots and Systems* (pp. 3343–3348). IEEE.
- 264 Ferguson, R. L., Christensen, P. R., & Kieffer, H. H. (2006). High-resolution thermal inertia derived from
265 the thermal emission imaging system (themis): Thermal model and applications. *Journal of Geophysical
266 Research: Planets*, 111.
- 267 Fong, T., Seabloom, M., Furlong, M., & Tan, F. (2017). Workshop on autonomy for future smd missions, .
- 268 Gaines, D., Anderson, R., Doran, G., Huffman, W., Justice, H., Mackey, R., Rabideau, G., Vasavada, A.,
269 Verma, V., Estlin, T. et al. (2016). Productivity challenges for mars rover operations, .
- 270 Golombek, M., & Rapp, D. (1996). Size-frequency distributions of rocks on mars. In *Lunar and Planetary
271 Science Conference*. volume 27.
- 272 Helmick, D., Angelova, A., Matthies, L., Brooks, C., Halatci, I., Dubowsky, S., & Iagnemma, K. (2008).
273 Experimental results from a terrain adaptive navigation system for planetary rovers. In *the Ninth Inter-
274 national Symposium on Artificial Intelligence, Robotics and Automation in Space, i-SAIRAS*.
- 275 Heverly, M., Matthews, J., Lin, J., Fuller, D., Maimone, M., Biesiadecki, J., & Leichty, J. (2013). Traverse
276 performance characterization for the mars science laboratory rover. *Journal of Field Robotics*, 30, 835–846.
- 277 Iagnemma, K., Kang, S., Shibly, H., & Dubowsky, S. (2004). Online terrain parameter estimation for wheeled
278 mobile robots with application to planetary rovers. *IEEE transactions on robotics*, 20, 921–927.
- 279 Johnson, J. B., Kulchitsky, A. V., Duvoy, P., Iagnemma, K., Senatore, C., Arvidson, R. E., & Moore, J.
280 (2015). Discrete element method simulations of mars exploration rover wheel performance. *Journal of
281 Terramechanics*, 62, 31–40.
- 282 Lindemann, R. A., & Voorhees, C. J. (2005). Mars exploration rover mobility assembly design, test and
283 performance. In *2005 IEEE International Conference on Systems, Man and Cybernetics* (pp. 450–455).
284 IEEE volume 1.
- 285 Liu, X.-Y., Wu, J., & Zhou, Z.-H. (2008). Exploratory undersampling for class-imbalance learning. *IEEE
286 Transactions on Systems, Man, and Cybernetics, Part B (Cybernetics)*, 39, 539–550.
- 287 Lorenz, R. D., Turtle, E. P., Barnes, J. W., Trainer, M. G., Adams, D. S., Hibbard, K. E., Sheldon, C. Z.,
288 Zacny, K., Peplowski, P. N., Lawrence, D. J. et al. (2018). Dragonfly: a rotorcraft lander concept for
289 scientific exploration at titan. *Johns Hopkins APL Technical Digest*, 34, 374–387.
- 290 Maimone, M., Cheng, Y., & Matthies, L. (2007). Two years of visual odometry on the mars exploration
291 rovers. *Journal of Field Robotics*, 24, 169–186.
- 292 Muro, T. (2004). *Terramechanics: land locomotion mechanics*. CRC Press.
- 293 NASA (2018). <https://www.nasa.gov/press-release/nasa-announces-landing-site-for-mars-2020-rover>.
- 294 Ono, M., Heverly, M., Rothrock, B., Almeida, E., Calef, F., Soliman, T., Williams, N., Gengl, H., Ishimatsu,
295 T., Nicholas, A. et al. (2018). Mars 2020 site-specific mission performance analysis: Part 2. surface
296 traversability. In *2018 AIAA SPACE and Astronautics Forum and Exposition* (p. 5419).
- 297 Ono, M., Rothrock, B., Almeida, E., Ansar, A., Otero, R., Huertas, A., & Heverly, M. (2016). Data-driven
298 traverability analysis for mars 2020 landing site selection, .
- 299 Papadakis, P. (2013). Terrain traversability analysis methods for unmanned ground vehicles: A survey.
300 *Engineering Applications of Artificial Intelligence*, 26, 1373–1385.

- 301 Putzig, N. E., & Mellon, M. T. (2007). Apparent thermal inertia and the surface heterogeneity of mars.
302 *Icarus*, 191, 68–94.
- 303 Putzig, N. E., Mellon, M. T., Kretke, K. A., & Arvidson, R. E. (2005). Global thermal inertia and surface
304 properties of mars from the mgs mapping mission. *Icarus*, 173, 325–341.
- 305 Rothrock, B., Kennedy, R., Cunningham, C., Papon, J., Heverly, M., & Ono, M. (2016). Spoc: Deep
306 learning-based terrain classification for mars rover missions. In *AIAA SPACE 2016* (p. 5539).
- 307 Sebastián, E., Armiens, C., Gómez-Elvira, J., Zorzano, M. P., Martínez-Frias, J., Esteban, B., & Ramos,
308 M. (2010). The rover environmental monitoring station ground temperature sensor: A pyrometer for
309 measuring ground temperature on mars. *Sensors*, 10, 9211–9231.
- 310 Seiffert, C., Khoshgoftaar, T. M., Van Hulse, J., & Napolitano, A. (2008). Rusboost: Improving classification
311 performance when training data is skewed. In *2008 19th International Conference on Pattern Recognition*
312 (pp. 1–4). IEEE.
- 313 Seiffert, C., Khoshgoftaar, T. M., Van Hulse, J., & Napolitano, A. (2009). Rusboost: A hybrid approach to
314 alleviating class imbalance. *IEEE Transactions on Systems, Man, and Cybernetics-Part A: Systems and*
315 *Humans*, 40, 185–197.
- 316 Senatore, C., Stein, N., Zhou, F., Bennett, K., Arvidson, R., Trease, B., Lindemann, R., Bellutta, P.,
317 Heverly, M., & Iagnemma, K. (2014). Modeling and validation of mobility characteristics of the mars
318 science laboratory curiosity rover. In *Proc. Proceedings of the 12th International Symposium on Artificial*
319 *Intelligence, Robotics and Automation in Space (i-SAIRAS)*.
- 320 Weiss, G. M. (2004). Mining with rarity: a unifying framework. *ACM Sigkdd Explorations Newsletter*, 6,
321 7–19.
- 322 Wong, J. Y. et al. (1989). *Terramechanics and off-road vehicles*. Elsevier.
- 323 Zacny, K., Wilson, J., Craft, J., Asnani, V., Oravec, H., Creager, C., Johnson, J., & Fong, T. (2010). Robotic
324 lunar geotechnical tool. In *Earth and Space 2010: Engineering, Science, Construction, and Operations in*
325 *Challenging Environments* (pp. 166–181).
- 326 Zhou, F., Arvidson, R., & Zastrow, A. (2017). Simulating mars science laboratory curiosity rover traverses
327 using artemis. In *Lunar and Planetary Science Conference*. volume 48.
- 328 Zhou, F., Arvidson, R. E., Bennett, K., Trease, B., Lindemann, R., Bellutta, P., Iagnemma, K., & Senatore,
329 C. (2014). Simulations of mars rover traverses. *Journal of Field Robotics*, 31, 141–160.